Citation: CPT Pharmacometrics Syst. Pharmacol. (2017) 6, 614–624; doi:10.1002/psp4.12221

ORIGINAL ARTICLE

Population Pharmacokinetic and Pharmacodynamic Modeling of LY2510924 in Patients With Advanced Cancer

S Bihorel[1], E Raddad[2]*, J Fiedler-Kelly[1], JR Stille[2], J Hing[1] and E Ludwig[1]

The objectives of this study were to characterize the pharmacokinetics (PK) of LY2510924, a potent peptide antagonist of the CXCR4 receptor, after subcutaneous administration in patients with advanced cancer forms and quantify LY2510924 stimulatory effects on the mobilization of cells bearing the cluster of differentiation 34 (CD34) as an indirect reflection of the chemokine C-X-C motif ligand 12/CXCR4 axis inhibition. LY2510924 PK were best characterized by a two-compartment model with first-order absorption and dose-dependent clearance predicting steady state after three daily doses and little accumulation (accumulation ratio <1.17). The dynamics of CD34+ cell counts were best characterized with a precursor model with reversible transfer from the precursor to the central compartment and LY2510924-driven stimulation of cell mobilization. Model-based simulations show that once-daily doses of 20 mg LY2510924 produce maximum CD34+ cell response and that peak effect typically occurs after three daily doses and slowly wanes over time.
CPT Pharmacometrics Syst. Pharmacol. (2017) **6**, 614–624; doi:10.1002/psp4.12221; published online 23 June 2017.

Study Highlights

WHAT IS THE CURRENT KNOWLEDGE ON THE TOPIC?

☑ LY2510924 is a peptide antagonist of the CXC receptor 4, which is overexpressed in a variety of cancers and involved in tumor metastasis. Data on LY2510924 pharmacokinetics (PK) and its effect on blood CD34+ cell counts have been only partially published, and no quantitative PK or pharmacokinetic/pharmacodynamic (PK/PD) model is currently available in the literature for this drug.

WHAT QUESTION DID THIS STUDY ADDRESS?

☑ This study quantitatively explores the relationships between LY2510924 dose, plasma concentrations, and blood CD34+ cell counts.

WHAT THIS STUDY ADDS TO OUR KNOWLEDGE

☑ The PK model predicts the concentrations of LY2510924 for various doses of the drug. The PK/PD model predicts the CD34+ cell response to repeated LY2510924 dosing.

HOW MIGHT THIS CHANGE DRUG DISCOVERY, DEVELOPMENT, AND/OR THERAPEUTICS?

☑ The proposed models provide quantitative tools to support decision-making for further development of LY2510924.

The vast majority of deaths in cancer patients can be attributed to secondary metastases rather than to the primary tumors. Therefore, the development of agents targeting the biological processes that promote or mediate metastasis may provide significant improvement in the care and survival of cancer patients.

Binding of the chemokine C-X-C motif ligand 12 (CXCL12; also known as stromal-cell derived factor-1 (SDF-1)), to the G-protein transmembrane CXC receptor 4 (CXCR4), is involved in normal organogenesis and embryogenesis, as well as tissue homeostasis by regulation of cell homing and trafficking.[1] CXCL12 concentration gradients drive the recruitment of CXCR4+ cells, such as lymphocytes or hematopoietic progenitors, and promote their migration to and retention in tissues with a high CXCL12 expression level, such as bone, liver, and lungs. Conversely, mobilization of progenitors to the bloodstream, monitored using counts of cells bearing the cluster of differentiation 34 (CD34),[2] is increased by administration of CXCR4 antagonists.[3,4]

The CXCL12/CXCR4 axis is also believed to play a significant role in the regulation of organ-specific metastasis, tumor growth, invasion, survival, and angiogenesis.[5] Overexpression of CXCR4 has been reported in 23 different types of cancer cells in humans,[1] including renal cell carcinoma (RCC) and small cell lung carcinoma (SCLC).[6,7] Stromal cells in tissues such as bone, brain, liver, and lungs secrete CXCL12, inducing the migration of CXCR4-expressing cancer cells toward these tissues.

LY2510924 is a potent and selective 1189.5-Da peptide antagonist of CXCR4.[8] LY2510924 was shown *in vitro* to inhibit CXCL12 binding to human CXCR4 in a dose-dependent manner with a half-inhibitory concentration of ~0.08–0.3 nM, depending on the cell line. LY2510924 also

[1]Cognigen Corporation, a Simulations Plus Company, Buffalo, New York, USA; [2]Chorus, Lilly Research Laboratories, Eli Lilly and Company, Indianapolis, Indiana, USA. *Corresondence: Eyas Raddad (eyas@lilly.com)
Received 23 May 2017; accepted 12 June 2017; published online on 23 June 2017. doi:10.1002/psp4.12221

inhibits CXCL12/CXCR4-mediated GTP binding, downstream cell-signaling, and chemotaxis activities in the 0.2–4 nM range and does not exhibit any CXCR4 agonist properties. Furthermore, LY2510924 administration in rodent and primate models resulted in dose- and time-dependent mobilization of leukocytes and hematopoietic progenitors to the blood stream. LY2510924 also demonstrated dose-dependent inhibition activity on tumor growth in human xenograft models developed with non–Hodgkin lymphoma, RCC, lung, and colon cancer cells that express functional CXCR4. Significant tumor suppression was seen at doses resulting in a 6-fold increase in blood progenitor cell counts in C57B mice. Additionally, in an MDA-MB-231 breast cancer metastatic xenograft model, LY2510924 administration was demonstrated to inhibit tumor metastasis.[8]

LY2510924 pharmacokinetics (PK) in humans are characterized by rapid absorption after subcutaneous (s.c.) injections and non-dose-proportional disposition.[9] Preclinical evaluations suggested that LY2510924 undergoes metabolic degradation, but is not a substrate, an inhibitor, or an inducer of cytochromes. Excretion studies in rats showed that $<$40% of the dose is recovered as parent drug in urine.

This report describes the development of fit-for-purpose population models for the PK and pharmacokinetics/pharmacodynamics (PK/PD) of LY2510924 using nonlinear mixed effects analysis of data collected after repeated s.c. injections in patients with advanced and/or metastatic cancers.[9–11] The inhibitory activity of LY2510924 on the CXCL12-CXCR4 axis was assessed in the PK/PD model by following the changes in blood CD34+ cell counts (CCC).

METHODS

Study designs, dosing regimens, and subjects

Data used to perform this population analysis were collected from three open-label clinical studies: I2V-MC-CXAA, I2V-MC-CXAB, and I2V-MC-CXAC, hereafter referred to as Studies CXAA, CXAB, and CXAC. All study participants received one or more cycles of LY2510924 administered as once-daily s.c. injections, according to study-specific dosing schemes (see **Supplementary Information**). Actual time of sampling and dosing events for LY2510924 and standard of care (SoC) comedications were used in the dataset. Delays and lapses in LY2510924 dosing were captured and were associated with delays in SoC dosing.

Study CXAA was a nonrandomized, dose-escalation, phase I study in patients with advanced metastatic cancer for whom no treatment of higher priority existed.[9] Study CXAA consisted of a dose-escalation phase followed by a dose-confirmation phase. In the dose-escalation phase, 3–6-patient cohorts were treated with once-daily s.c. LY2510924 doses ranging from 1–30 mg/day for 28 days with intervals of up to 7 days between treatment cycles. Dose escalation to the next level was determined by investigators and the Sponsor medical monitor based on safety, PK, and PD data. In the dose-confirmation phase, 10-patient cohorts were treated with daily LY2510924 doses of 2.5 or 20 mg/day for 28 days with intervals of up to 7 days between treatment cycles. In both phases, samples for measurement of plasma LY2510924 concentrations and blood CCC were collected using a rich sampling scheme (see **Supplementary Information**).

Study CXAB was a randomized, active-controlled, phase II study in patients with metastatic RCC who did not receive prior treatment for RCC.[10] Patients were randomized 2:1 to receive LY2510924 with the SoC treatment of sunitinib (arm A) or only sunitinib (arm B). Daily s.c. injections of 20 mg LY2510924 were administered without interruption during the 6-week treatment cycles, while sunitinib was only administered during the first 4 weeks as a daily 50-mg oral dose. There was typically no interruption between treatment cycles.

Study CXAC was a randomized, active-controlled, phase II study in patients with extensive-stage SCLC who did not receive prior treatment for SCLC.[11] Patients were randomized 1:1 to receive LY2510924 with the SoC treatment of etoposide and carboplatin (arm A) or only the SoC treatment (arm B). Daily s.c. injections of 20 mg LY2510924 were administered during the first week of the 21-day treatment cycles, while a single intravenous (i.v.) injection of carboplatin was given on the first day of each cycle at individualized doses targeting an area under the curve of 5 mg/mL/min and daily i.v. injections of 100 mg/m^2 etoposide were administered on the first 3 days of each cycle.

In both CXAB and CXAC studies, a sparse sampling scheme was used to collect PK samples in arm A and PD samples in both study arms (see **Supplementary Information**).

In all studies, serum samples were collected at multiple times prior to and after initiation of LY2510924 administration to test for the development of antidrug antibodies (ADA).

All study protocols and consent forms were reviewed and approved by Institutional Review Boards at each of the research sites. Before entering the studies, all subjects were informed about the risks of the studies and signed an informed consent form, according to the recommendations of the Declaration of Helsinki.

Bioanalytical methods

LY2510924 concentrations were determined in plasma samples using a validated liquid chromatography-tandem mass spectroscopy method, with lower and upper limits of quantification of 0.2 and 100 ng/mL.

Blood samples were analyzed for CCC using a flow cytometry method, with lower limits of quantification of 0.5 cells/μL.

Qualitative detection of ADA was performed using a direct enzyme-linked immunosorbent assay, based on ADA capture by LY2510924 immobilized on a plate and detection using horseradish peroxidase-conjugated goat antihuman immunoglobulins (Ig) G, M, and A. The complex was visualized using a SureBlue tetramethylbenzidine substrate (KPL, Gaithersburg, MD). Negative control was a pooled normal human serum. Serum from cynomolgus monkeys hyperimmunized with LY2510924 was used at various dilutions as the positive control. LY2510924 concentrations $\geq$1 μg/mL interfered with this assay, which was not considered drug tolerant. However, concentrations

were significantly lower than 1 μg/mL at the times of sampling for ADA testing.

Analysis software

NONMEM v. 7.3.0 was used to develop nonlinear mixed effects models for LY2510924 PK and its effect on CCC dynamics.[12] Tabular and graphical data displays were created with KIWI v. 1.5[13] and SAS v. 9.2 (SAS Institute, Cary, NC). Statistics supporting the creation of visual predictive check (VPC) plots were generated with Perl-Speaks-NONMEM v. 4.4.0.[14]

PK and PK/PD model development

Structural models for LY2510924 PK and PK/PD were first evaluated using the richly sampled data obtained in Study CXAA. In a second stage, the models were refined when the sparse data collected in Studies CXAB and CXAC became available. A sequential approach using one of two methods (population PK parameters and data or individual PK parameters)[15] was applied to develop the PK/PD model for CCC dynamics. Selection of PK and PK/PD models was based on the goodness-of-fit plots, successful outcomes of the estimation and covariance routines, and the reasonableness and precision of the parameter estimates. Interindividual variability (IIV) was described using exponential variability models combined in a simple diagonal matrix form or in a partial variance-covariance matrix. Various residual variability (RV) models were tested, including constant coefficient of variation (CCV) and additive plus CCV models.

Various PK model structures were explored including two- and three-compartment mammillary models with fixed or estimated first-order absorption and first-order or dose-dependent elimination. Although no formal covariate analysis was performed, the effect of body weight on PK parameters was assessed during the second stage of PK model development using allometric power relationships with fixed or estimated coefficients, for reasons provided in the Discussion.

Indirect response models with stimulation of CD34+ cell production or inhibition of CD34+ cell elimination[16] were initially explored to describe the effect of LY2510924 on CCC in Study CXAA. Precursor-dependent indirect response models[17] were also evaluated using various combinations of the following cell dynamics and drug effect features: recycling of CD34+ cell back to the precursor pool, linear or nonlinear elimination of CD34+ cells, negative feedback of CCC on cell production, stimulation of CD34+ transfer from the pool to the response compartment, inhibition of CD34+ cell elimination or recycling to the precursor pool, and time-dependent stimulation of LY2510924 effects. Due to the limited knowledge regarding the CD34+ cell life cycle and the LY2510924 influence on it, the aforementioned components were empirically tested for their ability to describe CCC data patterns rather than mechanistically motivated.

The effect of SoC and concomitant use of erythropoietin (EPO, as epoetin alfa or darbapoietin) and/or granulocyte-colony stimulating factor (G-CSF, as filgrastim or pegfilgrastim) on CD34+ cell dynamics was evaluated based on data collected in Studies CXAB and CXAC. These effects were tested on CD34+ production or mobilization rates and implemented as simple shifts, stimulations by empirical signal build-up over time, or driven by SoC or comedication dosing. In the latter case, the kinetics of the SoC medications, EPO, and G-CSF were simplified using a kinetic-pharmacodynamic (KPD) modeling approach, since concentrations of these drugs were not measured.[18] It should be noted that due to the differences in population and design across studies, the effects of SoC, cancer type, and study could not be distinguished.

Final models were evaluated using a simulation-based VPC method with (for PK) or without (for PK/PD) prediction-correction,[19] a technique that normalizes the observed and simulated data based on the typical population prediction, thus enhancing the ability to diagnose model misspecifications.

Finally, deterministic simulations were performed to predict the PK and PD responses in a typical 80.1-kg patient after daily administration of various LY2510924 doses over 28 days.

RESULTS

A total of 767 LY2510924 plasma samples collected from 147 patients (including 473 samples collected using a rich sampling scheme in 40 patients enrolled in Study CXAA) were used in the population PK analysis. A total of 1,042 CCC collected from 227 patients (including 367 samples collected using a rich sampling scheme in 39 patients enrolled in Study CXAA) were used in the population PK/PD analysis. Demographics and baseline CCC from patients included in the analyses are summarized in **Table 1**. It should be noted that some patients who only had baseline CCC measurements were included in the PK/PD analysis, but not in the PK analysis. While the distribution of patient pathology in Studies CXAB and CXAC was well defined due to the specific inclusion criteria, patients enrolled in Study CXAA were diagnosed with a broad variety of cancer types affecting mostly the gastrointestinal tract (46.2%), lungs (15.4%), and the genitourinary system (12.8%), with limited commonality with the pathologies observed in Studies CXAB and CXAC. A small fraction of the patients in Studies CXAB and CXAC received concomitant EPO and/or G-CSF.

None of the patients included in the analysis datasets developed ADA.

Pharmacokinetic model for LY2510924

A two-compartment model with first-order absorption and dose-dependent clearance best described the PK of LY2510924 (**Figure 1**). The addition of a third peripheral compartment did not significantly improve model performance. The apparent elimination clearance (CL/F) was allometrically scaled to body weight (*WTKG*) and related to the LY2510924 dose using a decreasing sigmoid function defined as follows:

Table 1 Summary of patient characteristics by study and treatment arm

Subject characteristic		I2V-MC-CXAA	I2V-MC-CXAB		I2V-MC-CXAC		
		LY2510924	LY2510924 + SoC	SoC	LY2510924 + SoC	SoC	Overall
Age (y)	Mean (SD)	64.4 (9.6)	64.1 (11.4)	63.2 (9.2)	63.2 (9.1)	66.7 (8.1)	64.3 (9.8)
	Range	41, 85	29, 83	41, 76	46, 84	47, 85	29, 85
	n	39	70	30	47	41	227
Baseline weight (kg)	Mean (SD)	79.40 (20.50)	87.50 (20.90)	92.00 (26.80)	80.80 (21.60)	82.40 (20.60)	84.40 (22.00)
	Range	39.6, 152.0	49.3, 136.5	53.5, 167.8	47.6, 144.2	45.5, 134.3	39.6, 167.8
	n	39	70	30	47	41	227
Baseline CD34+ cell count (cells/μL)	Mean (SD)	1.7 (1.4)	1.8 (1.7)	1.8 (1.2)	2.1 (1.9)	1.7 (1.6)	1.8 (1.6)
	Range	0, 7	0, 13	0, 5	1, 11	0, 9	0, 13
	n	39	66	26	42	38	211
Sex, *n* (%)	Male	21 (53.8)	46 (65.7)	20 (66.7)	22 (46.8)	17 (41.5)	126 (55.5)
	Female	18 (46.2)	24 (34.3)	10 (33.3)	25 (53.2)	24 (58.5)	101 (44.5)
Ethnicity, *n* (%)	Caucasian	31 (79.5)	66 (94.3)	28 (93.3)	43 (91.5)	38 (92.7)	206 (90.7)
	Black/African American	6 (15.4)	4 (5.7)	2 (6.7)	3 (6.4)	2 (4.9)	17 (7.5)
	American Indian/ Alaskan Native	0 (0.0)	0 (0.0)	0 (0.0)	1 (2.1)	0 (0.0)	1 (0.4)
	Unknown	2 (5.1)	0 (0.0)	0 (0.0)	0 (0.0)	1 (2.4)	3 (1.3)
Cancer type, *n* (%)	Renal Cell Carcinoma	1 (3.6)	70 (100.0)	30 (100.0)	0 (0.0)	0 (0.0)	101 (44.5)
	Small Cell Lung Carcinoma	0 (0)	0 (0.0)	0 (0.0)	47 (100)	41 (100.0)	88 (38.8)
	Other[a]	38 (97.4)	0 (0.0)	0 (0.0)	0 (0.0)	0 (0.0)	38 (16.7)
ADA status, *n* (%)	Positive	0 (0.0)	0 (0.0)	0 (0.0)	0 (0.0)	0 (0.0)	0 (0.0)
	Negative	39 (100.0)	70 (100.0)	30 (100.0)	47 (100.0)	41 (100.0)	227 (100.0)
G-CSF use, n(%)	Yes	0 (0.0)	0 (0.0)	0 (0.0)	12 (25.5)	16 (39.0)	28 (12.3)
	No	39 (100.0)	70 (100.0)	30 (100.0)	35 (74.5)	25 (61.0)	199 (87.7)
EPO use, *n* (%)	Yes	0 (0.0)	3 (4.3)	0 (0.0)	1 (2.1)	2 (4.9)	6 (2.6)
	No	39 (100.0)	67 (96.7)	30 (100.0)	46 (97.9)	39 (95.1)	221 (97.4)

ADA, antidrug antibodies, EPO, erythropoietin; G-CSF, granulocyte-colony stimulating factor; *n*, number of patients; SD, standard deviation.
[a]Other types include cancers of the gastrointestinal tract ($n = 18$), lungs ($n = 6$), genitouninary system ($n = 5$), breasts ($n = 2$), thyroid ($n = 1$), and mesothelioma ($n = 4$), lymphoma ($n = 1$), and sarcoma ($n = 1$).

$$CL/F(dose) = \left(\frac{WTKG}{80.1}\right)^{b_{CL}} \times \begin{cases} TVCL_{\min}/F + TVCL_{delta}/F, & dose \leq 1 \text{ mg} \\ TVCL_{\min}/F + TVCL_{delta}/F - \dfrac{TVCL_{delta}/F \times (dose - 1)}{(dose_{50} - 1) + (dose - 1)}, & dose > 1 \text{ mg} \end{cases} \quad (1)$$

where b_{CL} is the estimated typical allometric exponent for clearance, $TVCL_{delta}/F$ is the typical difference between the typical minimum apparent elimination clearance ($TVCL_{\min}/F$) and the typical maximum apparent elimination clearance, and $dose_{50}$ is the typical half-inhibitory dose (i.e., the LY2510924 dose at which CL/F reaches half of its possible range or $\left(\frac{WTKG}{80.1}\right)^{b_{CL}} \times (TVCL_{\min}/F + 0.5 \times TVCL_{delta}/F)$. All typical parameters are relative to an 80.1-kg subject (i.e., the median body weight in the analysis population).

The apparent central volume of distribution ($V2/F$) was also allometrically scaled to individual body weight as follows:

$$V2/F = TVV2/F \times \left(\frac{WTKG}{80.1}\right)^{b_V} \quad (2)$$

where $TVV2/F$ is the typical apparent central volume of distribution in an 80.1-kg subject and b_V is the estimated typical allometric exponent for central volume.

Interindividual variability in CL/F and $V2/F$ was defined as follows for subject i:

$$CL_i/F = CL/F \times e^{\eta_{CL,i}} \quad (3)$$

$$V2_i/F = V2/F \times e^{\eta_{V2,i}} \quad (4)$$

where $\eta_{CL,i}$ and $\eta_{V2,i}$ are the Bayesian estimates of random variability in CL/F and $V2/F$, respectively. RV was estimated using separate additive plus CCV error models for phase I and phase II studies.

No allometric scaling component was included in the initial model based on Study CXAA data. Good agreement

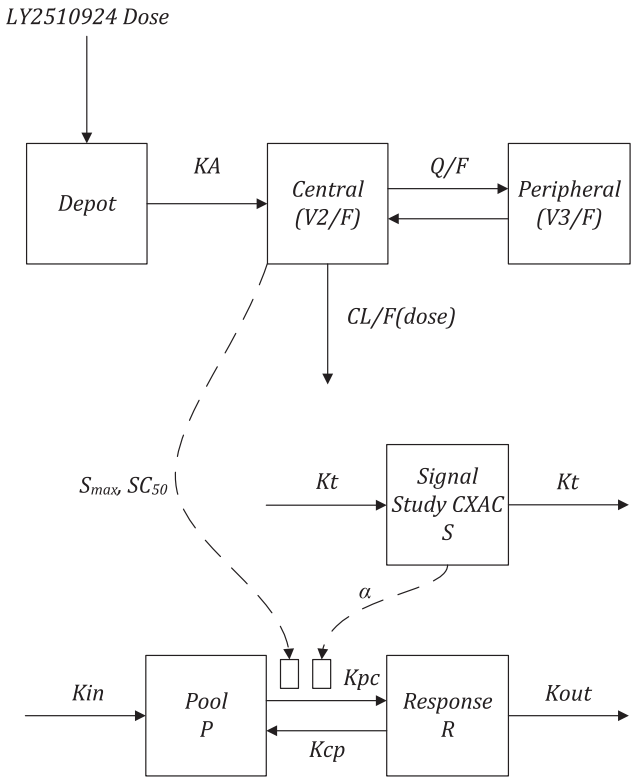

Figure 1 Diagram of the pharmacokinetic/pharmacodynamic model for LY2510924. $\propto$, signal stimulatory factor; *CL*/*F*, apparent elimination clearance; *KA*, first-order rate of absorption; *Kcp*, first-order rate of transfer of CD34+ cells from the response back to the pool compartment; *Kin*, CD34+ cell production into the precursor compartment; *Kpc*, first-order rate of transfer of CD34+ cells from the pool to the response compartment; *Kout*, first-order rate of CD34+ cell elimination; *Kt*, first-order signal transit rate; *Q*/*F*, apparent distribution clearance; SC_{50}, LY2510924 concentration at which half of the maximum stimulatory effect is achieved; S_{max}, the maximum stimulatory effect of LY2510924; *V*2/*F*, apparent central volume of distribution; *V*3/*F*, apparent peripheral volume of distribution.

was obtained between model predictions and observed data from each study when this base model was extended to the pooled data from Studies CXAA, CXAB, and CXAC. However, refinements were required to further improve this re-estimated model. Body weight-based allometric scaling was introduced for *CL*/*F* and *V*2/*F* to eliminate positive correlations between body size descriptors and the IIV terms associated with these parameters. The allometric coefficients were reasonably close to standard values (i.e., 0.870 vs. 0.75 for *CL*/*F* and 0.948 vs. 1 for *V*2/*F*)[20] and, overall, the magnitude of unexplained variability associated with *CL*/*F* and *V*2/*F* decreased by 5.7%CV and 6.8%CV. This model refinement had no effect on the high correlation that was developed between the $dose_{50}$ and $TVCL_{min}/F$ estimates in the re-estimated model. In the final model, the $dose_{50}$ estimate was fixed to 3.6 mg, as this value was obtained from a base model estimation using Study CXAA data only, which provided the largest dose range and were, therefore, most informative to the estimation of $dose_{50}$.

All PK parameters were reasonably well estimated (**Table 2**). Overall, the model fit the data well based on the goodness-of-fit (GOF) (**Figure 2**, left column) and VPC plots (**Figure 3**).

Pharmacokinetic/pharmacodynamic model for LY2510924 effect on CD34+ cell counts

The changes in blood CCC were best described by a precursor-dependent indirect response model with reversible transfer of CD34+ cells from the pool to the response compartment to which CCC measurements are actually associated (**Figure 1**). In this model, the effect of LY2510924 was mediated by a saturable concentration-dependent stimulation of CD34+ cell mobilization to the response compartment. The model also included a second stimulatory process driven by a signal build-up over time for patients enrolled in Study CXAC. The change in CCC in the pool (*P*) and response (*R*) compartments and the dynamics of the stimulatory signal (*S*) were defined by the following system of differential equations:

$$\begin{aligned}
&\frac{dP}{dt} = Kin - Kpc \times \left(1 + \frac{S_{max} \times C_p}{SC_{50} + C_p} + \propto \times S\right) \times P + Kcp \times R, \\
&P(0) = CD34_0 \times \frac{Kout + Kcp}{Kpc} \\
&\frac{dR}{dt} = Kpc \times \left(1 + \frac{S_{max} \times C_p}{SC_{50} + C_p} + \propto \times S\right) \times P + (Kcp + Kout) \times R, \\
&R(0) = CD34_0 \\
&\frac{dS}{dt} = Kt \times F_{CXAC} \times (1 - S), \quad S(0) = 0
\end{aligned} \tag{5}$$

where $CD34_0$ is the estimated CCC at time zero, *Kpc* is the first-order rate of transfer of CD34+ cells from the pool to the response compartment, *Kcp* is the first-order rate of transfer of CD34+ cells from the response back to the pool compartment, *Kout* is the first-order rate of CD34+ cell elimination, *Kt* is the first-order signal transit rate, which is null for patients which were not enrolled in Study CXAC, S_{max} is the maximum stimulatory effect of LY2510924, SC_{50} is the LY2510924 concentration at which half of the maximum stimulatory effect is achieved, C_p is the LY2510924 concentration in the central compartment, $\propto$ is the signal stimulatory factor, and F_{CXAC} is set to 1 after the first dose for patients enrolled in Study CXAC and zero otherwise. Steady state with respect to CCC was assumed prior to the first dose of LY2510924 and/or SoC, and *Kin* was calculated as follows:

$$Kin = CD34_0 \times Kout \tag{6}$$

Interindividual variability was estimated for $CD34_0$, *Kout*, S_{max}, and SC_{50}, and RV was estimated using an additive plus proportional error model. All parameters were reasonably well estimated except *Kout* (**Table 2**). Overall, the model fit the data well, based on the GOF (**Figure 2,** right column) and VPC plots (**Figure 4**).

Table 2 Parameter estimates and standard errors for the final pharmacokinetic/pharmacodynamic model

	Final parameter estimate		Interindividual variability/residual variability	
Parameter	**Typical value**	**%SEM**	**Magnitude (shrinkage)**	**%SEM**
Pharmacokinetics				
$TVCL_{delta}/F$, L/h	12.9	11.1	29.8%CV	20.4
$TVCL_{min}/F$, L/h	4.75	7.09	(17.7%)	
$dose_{50}$, mg	3.60	FIXED		
b_{CL}	0.870	14.8		
$TVV2/F$, L	35.0	4.89	26.6%CV	32.5
b_V	0.948	14.8	(36.0%)	
TVQ/F, L/h	3.74	18.8	NE	NA
$TVV3/F$, L	21.9	6.67		
$TVKA$, h^{-1}	10.0	FIXED		
Phase 1 RV[a]	NE	NA	249 - 22.3%CV (6.71%)	
Phase 2 RV[a]			730 - 41.0%CV (13.8%)	
Pharmacodynamics				
$CD34_0$, cells/μL	1.45	5.66	75.6%CV (7.06%)	14.2
Kpc, 1000000/h	42.4	25.1	NE	NA
Kcp, h^{-1}	0.185	20.4		
$Kout$, h^{-1}	0.0104	51.1	220%CV (63.3%)	43.8
S_{max}	13.1	14.4	46.0%CV (48.0%)	52.4
SC_{50}, ng/mL	6.87	45.1	134%CV (62.1%)	63.8
Kt, h^{-1}	0.00804	15.5	NE	NA
∝	5.63	18.2	NE	NA
RV[b]	NE	NA	396 - 46.7%CV (11.9%)	

∝, stimulatory factor; %CV, coefficient of variation in percentage; %SEM, standard error of the mean in percentage; b_{CL}, typical allometric exponent specific to clearance; b_V, the typical allometric exponent specific to central volume; $CD34_0$, baseline CD34+ cell count; $dose_{50}$, half-inhibitory dose; Kcp, first-order rate of transfer of CD34+ cells from the response back to the pool compartment; $Kout$, first-order rate of CD34+ cell elimination; Kpc, first-order rate of transfer of CD34+ cells from the pool to the response compartment; Kt, first-order signal transit rate; NA, not applicable; NE, not estimated; SC_{50}, LY2510924 concentration at which half of the maximum stimulatory effect is achieved; S_{max}, the maximum stimulatory effect of LY2510924; $TVCL_{delta}/F$, typical difference between $TVCL_{min}/F$ and the typical maximum apparent elimination clearance; $TVCL_{min}/F$, typical minimum apparent elimination clearance; $TVKA$, typical first-order rate of absorption; TVQ/F, typical apparent distribution clearance; $TVV2/F$, typical apparent central volume of distribution; $TVV3/F$, typical apparent peripheral volume of distribution; RV, residual variability.

[a]The residual variability (%CV) was calculated for LY2510924 concentrations ranging from 0.2 to 25 ng/mL.

[b]The residual variability (%CV) was calculated for CD34+ cell counts ranging from 0.6 to 200 cells/μL.

DISCUSSION

This article describes the population modeling of LY2510924 PK in patients with various advanced types of cancer and the ability of LY2510924 to mobilize CD34+ cells to the peripheral blood compartment, as a marker of the drug pharmacological effect on the CXCL12/CXCR4 axis.

The selection of the structural model for LY2510924 PK was guided by the exploration of the densely collected data in Study CXAA. In previous noncompartmental analysis (NCA) of these data, LY2510924 was shown to exhibit a dose-dependent decrease in apparent elimination clearance, while apparent distribution volumes remained stable across doses.[9] Consistent with these results, nonlinear models with dose-dependent clearance (Eq. 1) better fit the Study CXAA data and corrected dose-dependent biases observed with the linear PK models initially tested, especially in the distribution of individual estimates of CL/F and $V2/F$. Equation 1 was defined with a positive lower boundary to ensure that CL/F cannot reach a nonphysiological null value. Additionally, the upper boundary of CL/F was defined relative to $TVCL_{min}/F$ rather than as an independent parameter to ensure that its value was always higher than the lower boundary and, thus, that Eq. 1 was a decreasing function of dose. Finally, the function was truncated at 1 mg, which

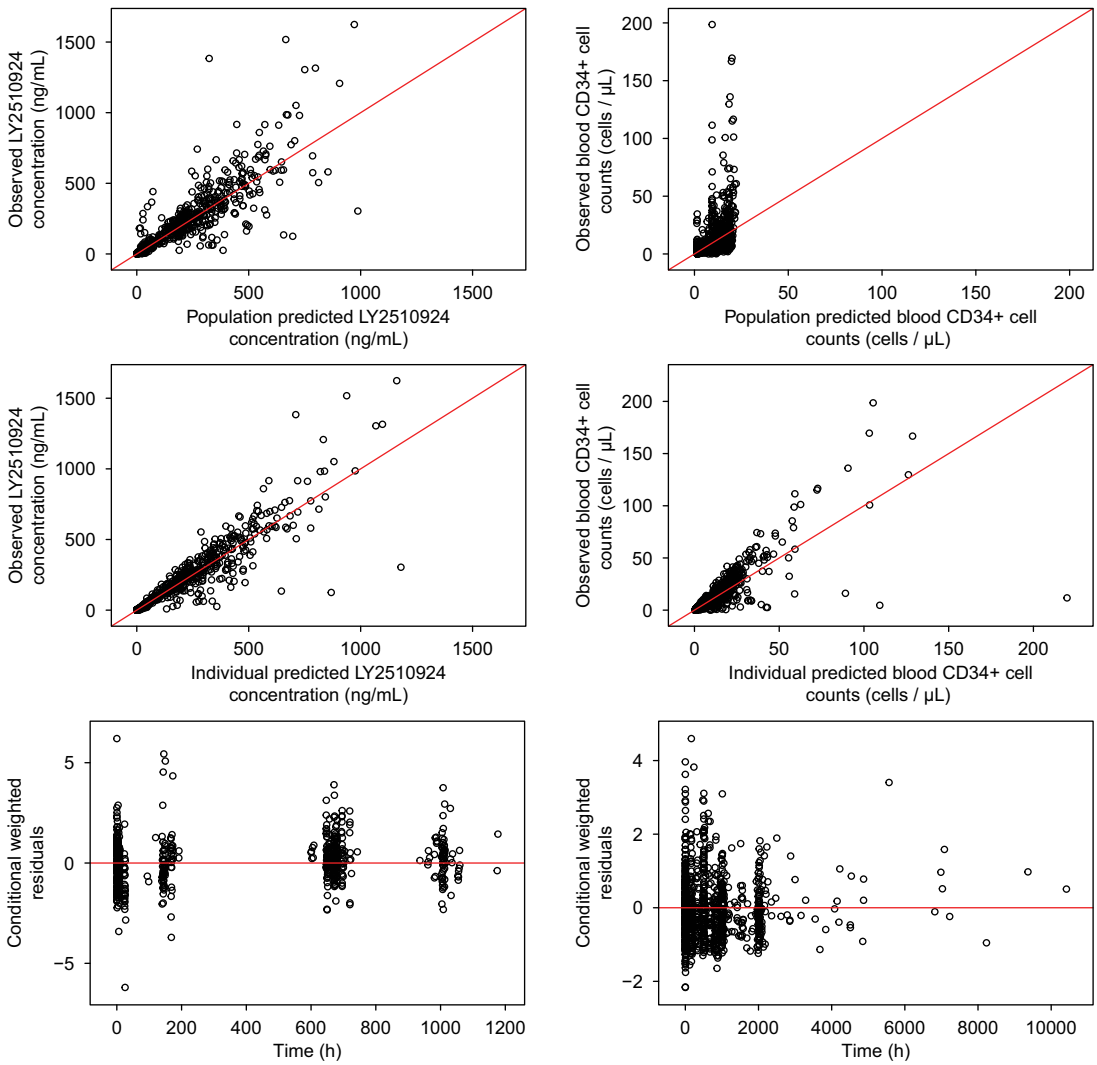

Figure 2 Goodness-of-fit plots for final LY2510924 pharmacokinetic and pharmacokinetic/pharmacodynamic model.

was the smallest LY2501924 dose tested and the dose providing the highest clearance estimate in previous NCA.[9]

Peak concentrations were typically observed by the first sampling time after dosing, indicating that LY2510924 absorption was fast relative to the sampling schedules applied in the different studies, including the rich sampling scheme in Study CXAA. Estimates of LY2510924 typical first-order absorption rate (*TVKA*) were high ($>$40 h^{-1}) and poorly estimated; therefore, *TVKA* was fixed to 10 h^{-1}, ensuring that absorption was more than 99% complete by the first nominal sampling time (i.e., 0.5 h after dosing, that is, $>$7 absorption half-lives). Alternative *TVKA* values resulted in higher objective function values for *TVKA* values $<$10 h^{-1} and no significant improvement for *TVKA* values $>$10 h^{-1}, while no significant changes in central and peripheral volume estimates were observed.

LY2510924 PK properties were similar to those generally observed in peptides. Fast absorption is typical for peptides below 1 kDa,[21] which are absorbed via the blood circulation and is consistent with LY2510924 molecular mass. Additionally, while peptides are generally degraded by peptidases, which are ubiquitously distributed throughout the body, some peptides, such as exenatide[22] or pegylated thrombopoeitin mimetic peptide,[23] exhibit nonlinear PK due to receptor-mediated uptake and intracellular metabolism. Although empirical, the model used to describe the dose-dependent decline in LY2510924 clearance down to a minimum value suggests a saturable and a nonsaturable mechanism acting simultaneously. We may hypothesize that binding to CXCR4 with subsequent uptake and degradation may play a role in the nonlinear elimination of LY2510924. Further investigation, however, is required to test this hypothesis.

Despite dose-dependent elimination, the PK model predicts little accumulation after daily dosing (**Figure 5c**) with typical accumulation ratio on day 28 ranging from 1.07–1.17 for doses between 2 and 50 mg/day. Further analyses are needed to determine if patient characteristics influence LY2510924 accumulation.

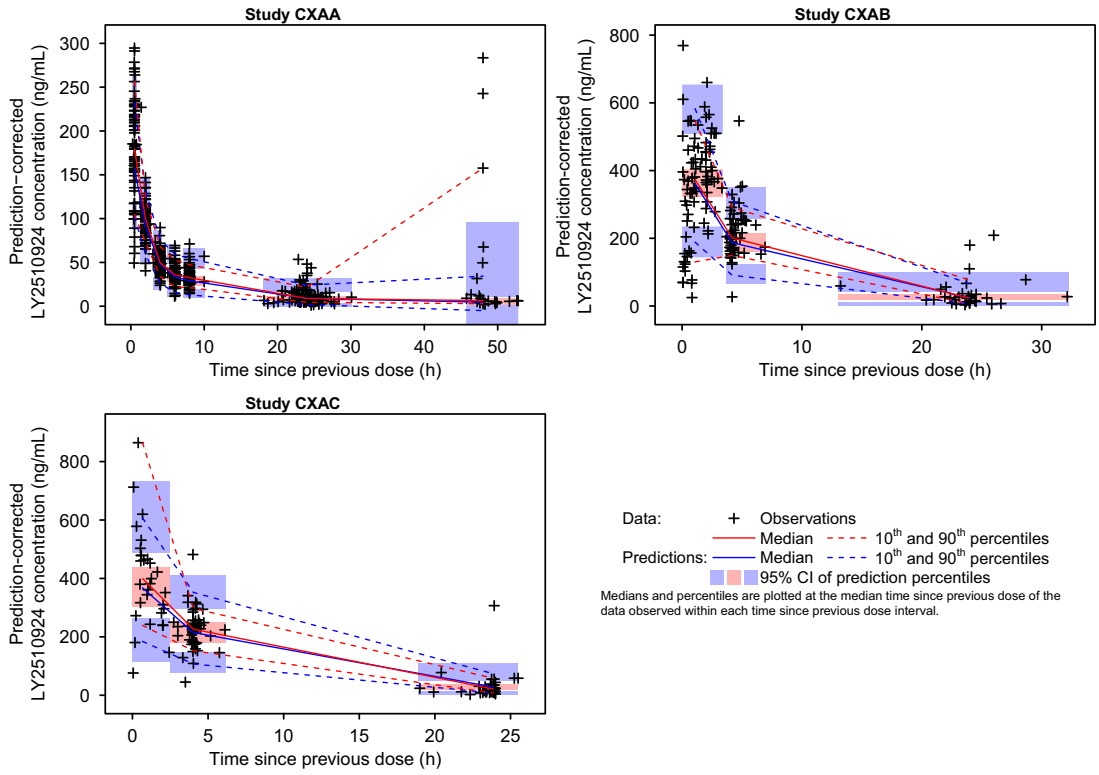

Figure 3 Visual predictive check plots for final pharmacokinetic model.

Previous reports have shown that LY2510924 engages its intended target at doses consistent with those administered in Studies CXAA, CXAB, and CXAC[9] and inhibits CXCL12/CXCR4-mediated cell signaling.[8] The CD34 antigen is a common marker of progenitor cells,[2] including (but not limited to) hematopoietic progenitor cells, which also express CXCR4[24] and are mobilized when the CXCL12/CXCR4 axis is perturbed. Therefore, blood CCC was selected as a biomarker for antagonist activity on the CXCL12/CXCR4 axis for LY2510924, as was done for other CXCR4 antagonists, including BTK140 and plerixafor.[3,4]

LY2510924 exerted a dose-dependent response in Study CXAA and caused a sustained, although variable, elevation in CCC. Average baseline-to-peak cell count increases as high as 5.5-fold were observed at 20 mg/day. However, the response was somewhat blunted by the end of the first 28-day treatment cycle. Differences in study design and sampling schedules in Studies CXAB and CXAC did not allow for direct comparison of baseline-to-peak cell counts with the Study CXAA results. Nevertheless, in the presence of LY2510924, maximum CCC increased on average 24.5-fold and 22.5-fold by the second treatment cycle in Studies CXAB and CXAC, respectively, compared to baseline values. While there was no noticeable increase in CCC between the first and second treatment cycle in the control arm of Study CXAB, maximum CCC increased on average 21.3-fold in the control arm of Study CXAC.

The structural model for LY2510924 effect on CD34+ cell dynamics was developed using the densely collected data in Study CXAA. Based on the previously proposed model of plerixafor effect on CD34+ mobilization,[25] simple indirect response models were initially tested. Although this type of model captured the LY2510924-driven increase in CCC, the late decline in CCC was not appropriately described. A precursor model structure with LY2510924-driven stimulation of cell transfer from the precursor to the central compartment (**Figure 1**) was then applied for its inherent ability to predict tolerance in drug effect[17] and its applicability to the process of CD34+ cell mobilization from tissues (predominantly the bone marrow) to the bloodstream. While many model variations were tested (see Methods section), model instability during optimization and poor convergence properties were only resolved by adding a component of CD34+ cell recycling back to the precursor pool to mimic tissue recapture of CD34+ cells.

The precursor model structure with cell recycling fit the data of Studies CXAA and CXAB reasonably well, but could not describe the rise in CCC observed in the control arm of Study CXAC, suggesting the implication of an LY2510924-independent stimulatory mechanism. We hypothesized that other medications, possibly G-CSF (see **Supplementary Information**), the SoC etoposide/carboplatin combination therapy, and/or EPO, were the cause of this LY2510924-independent increase in CCC. G-CSF is approved and is widely used for mobilizing autologous hematopoietic progenitor cells into the peripheral blood for the purpose of collection and allogeneic graft.[26,27] Similarly, a combination of etoposide, ifosfamide, and cisplatin was shown to promote a small mobilization of CD34+ cells in cancer patients.[28] Thus, attempts were made to model the influence of the

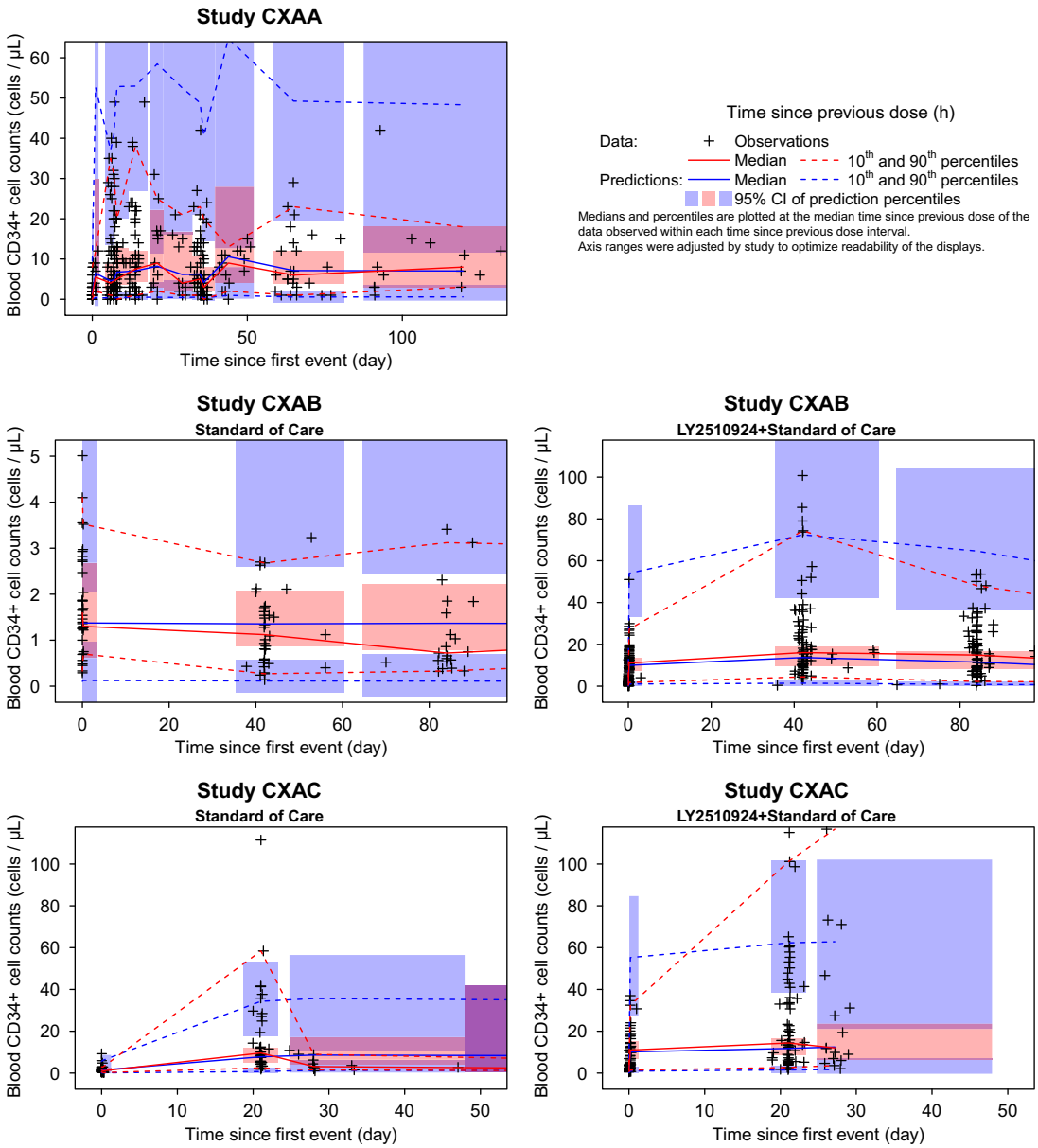

Figure 4 Visual predictive check plots for final pharmacokinetic/pharmacodynamic model.

SoC therapy, EPO, and/or G-CSF on the CD34+ cell production rate or mobilization rate using a time-varying covariate approach (in which the presence of comedication was associated with a proportional shift in the base rate) or using the dosing history in a KPD modeling approach.[18] These effects operated in both Study CXAC arms. Models with successful convergence resulted in unrealistically high stimulatory parameter estimates and poor predictive performance. The sampling schedule implemented in Study CXAC only provided CD34+ cell measurements at the beginning of two treatment cycles; therefore, we suspect that such sparse data and the high variability did not support the complexity of the tested models. Circadian fluctuations in CCC likely contributed to increased variability but could not be included in the models without data collected in the absence of drug.[29]

Improved model convergence and predictive properties were obtained by implementing simpler empirical model structures in which production or mobilization rates were stimulated by a signal build-up in patients enrolled in Study CXAC or were simply estimated to be different in Study CXAC. Typically, models in which the production rate was perturbed or different for Study CXAC patients showed good predictive performance, but exhibited very high shift or stimulatory parameter estimates and unrealistically long times to reach steady state (i.e., several hundred days), indicative of poor properties for extrapolation. In contrast, the selected model with a signal-driven stimulation of

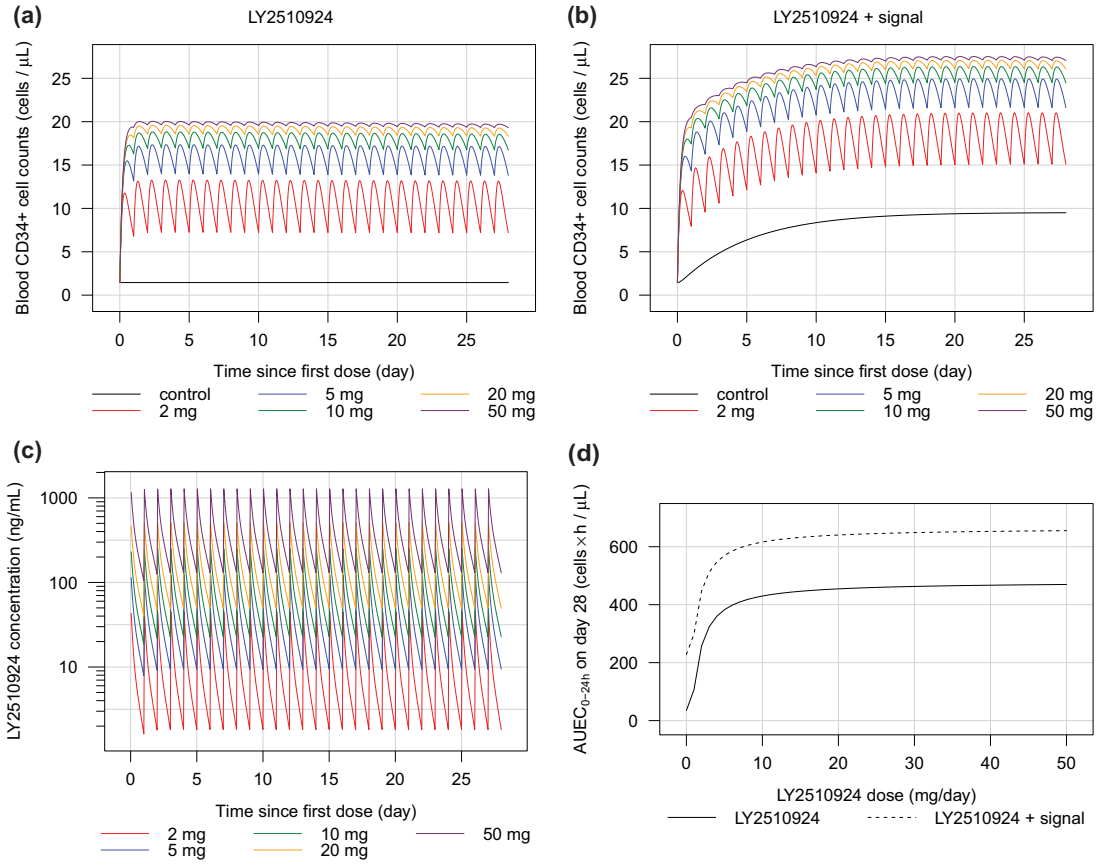

Figure 5 Predicted blood CD34+ cell count (**a,b**), LY2510924 plasma concentration (**c**), and daily area under the CD34+ cell count curve (**d**) following subcutaneous administration of LY2510924 for 28 days.

CD34+ mobilization resulted in realistic and generally reasonably well-estimated parameters and provided good predictive performance with a predicted steady-state effect within ~50 days of the first dose. No improvements were gained from implementing signal-driven stimulations on both CD34+ cell production and mobilization.

The authors acknowledge the largely empirical nature of the model component driving the CD34+ rise observed in Study CXAC patients and recognize its limitation for model simulation in the conditions of disease and concomitant therapy characterizing Study CXAC. However, additional data are likely required to implement a more mechanistic approach for the characterization of LY2510924-independent CCC rise in Study CXAC conditions. Overall, the selected model provided a reasonable description of the observed LY2510924 effect in all studies and estimated this effect to operate in the nanomolar range (i.e., SC_{50} of 6.87 ng/mL or 5.78 nM), which is consistent with the values observed in functional *in vitro* cell signaling (0.33–3.33 nM) or chemotaxis inhibition assays (0.26 nM).[8] Differences between clinical and preclinical experimental settings and the fact that SC_{50} reflects a plasma concentration rather than a concentration in tissues from which CD34+ cells are mobilized may have contributed to the slightly higher estimate of the inhibition constant.

Model-based simulations predict that typical LY2510924 concentrations are constantly above the estimated SC_{50} for doses as low as 5 mg/day (**Figure 5c**). Tolerance to LY2510924 appears to develop slowly and be of small predicted magnitude (**Figure 5a**). In addition, the empirical signal implemented for Study CXAC patients increased the typical CCC by 7 cells/μL and reaches steady state ~20 days after the start of the therapy (**Figure 5b**). Following a 28-day dosing period, near maximum effect is reached for an LY2510924 dose of 20 mg/day (**Figure 5d**). The relevance of the effect of LY2510924 on CCC to antitumor effect is not well understood. Thus, a 20-mg/day dose should not be interpreted as the dose that maximizes antitumor activity.

In conclusion, fit-for-purpose population models were successfully developed to characterize the PK of LY2510924 and its stimulatory effects on blood CCC following repeated s.c. dosing in patients with advanced forms of cancer, including SCLC and RCC. LY2510924 PK were best characterized by a two-compartment model with first-order absorption and dose-dependent clearance. The dynamics of CCC were best characterized with a precursor model with reversible transfer of cells from the precursor to the central compartment, LY2510924-driven stimulation of cell mobilization, and an empirical signal-driven stimulation of cell mobilization in patients enrolled in Study CXAC. Model-based simulation

confirmed that maximum CCC response is achieved with LY2510924 doses of 20 mg/day.

Conflict of Interest/Disclosure. Eyas Raddad and John R. Stille are employed by Eli Lilly & Company, which sponsors the development of LY2510924. Sébastien Bihorel, Jill Fiedler-Kelly, and Elizabeth Ludwig are employed by Cognigen Corporation and Jeremy Hing was employed by Cognigen Corporation at the time of this analysis. Cognigen Corporation was contracted by Eli Lilly & Company to perform the analysis reported in the current article.

Author Contributions. S.B., J.F-K., and E.L. wrote the article; E.J.R. and J.R.S. designed the research; S.B. and J.H. analyzed the data.

1. Chatterjee, S., Behnam Azad, B. & Nimmagadda, S. The intricate role of CXCR4 in cancer. *Adv. Cancer Res.* **124**, 31– 82 (2014).
2. Sidney, L.E., Branch, M.J., Dunphy, S.E., Dua, H.S. & Hopkinson A. Concise review: evidence for CD34 as a common marker for diverse progenitors. *Stem Cells.* **32**, 1380– 1389 (2014).
3. Peled, A. *et al.* The high-affinity CXCR4 antagonist BKT140 is safe and induces a robust mobilization of human CD34+ cells in patients with multiple myeloma. *Clin. Cancer Res.* **20**, 469– 479 (2014).
4. Cashen, A. *et al.* A phase II study of plerixafor (AMD3100) plus G-CSF for autologous hematopoietic progenitor cell mobilization in patients with Hodgkin lymphoma. *Biol. Blood Marrow Transplant.* **14**, 1253– 1261 (2008).
5. Cojoc, M. *et al.* Emerging targets in cancer management: role of the CXCL12/CXCR4 axis. *Oncol. Targets Ther.* **6**, 1347– 1361 (2013).
6. Li, G. *et al.* Prognostic value of CXCR4 expression in patients with clear cell renal cell carcinoma. *Histol. Histopathol.* **28**, 1217–1222 (2013).
7. Kijima, T. *et al.* Regulation of the cellular proliferation, cytoskeletal function and signal transduction through CXCR4 and c-Kit in small cell lung cancer cells. *Cancer Res.* **62**, 6304– 6311 (2002).
8. Peng, S.B. *et al.* Identification of LY2510924, a novel cyclic peptide CXCR4 antagonist that exhibits antitumor activities in solid tumor and breast cancer metastatic models. *Mol. Cancer Ther.* **14**, 480– 490 (2015).
9. Galsky, M.D. *et al.* A phase I trial of LY2510924, a CXCR4 peptide antagonist, in patients with advanced cancer. *Clin,. Cancer Res.* **20**, 3581– 3588 (2014).
10. Hainsworth, J.D. *et al.* A randomized, open-label phase 2 study of the CXCR4 inhibitor LY2510924 in combination with sunitinib vs. sunitinib alone in patients with metastatic renal cell carcinoma (RCC). *Target Oncol.* **11**, 643– 653 (2016).
11. Salgia, R. *et al*. A randomized phase II study of LY2510924 and carboplatin/etoposide vs. carboplatin/etoposide in extensive-disease small cell lung cancer. *Lung Cancer*. **105**, 7– 13 (2017).
12. Beal, S.L., Sheiner, L.B., Boeckmann, A.J. & Bauer, R.J. NONMEM User's Guides. Icon Development Solutions, Ellicott City, MD (1989–2014).
13. Bihorel, S. *et al.* KIWI: a collaborative platform for modeling and simulation. Poster presented at: Annual Meeting of the Population Approach Group in Europe (PAGE); 2014 Jun 10– 13; Alicante, Spain.
14. Lindbom, L., Pihlgren, P. & Jonsson, E.N. PsN-Toolkit—a collection of computer intensive statistical methods for nonlinear mixed effect modeling using NONMEM. *Comput. Methods Programs Biomed.* **79**, 241– 257 (2005).
15. Zhang, L., Beal, S.L. & Sheiner, L.B. Simultaneous versus sequential analysis for population PK/PD data I: best-case performance. *J. Pharmacokinet. Pharmacodyn.* **30**, 387– 404 (2003).
16. Sharma, A. & Jusko, W.J. Characterization of four basic models of indirect pharmacodynamic responses. *J. Pharmacokinet. Biopharm.* **24**, 611– 635 (1996).
17. Sharma, A., Ebling, W.F. & Jusko, W.J. Precursor-dependent indirect pharmacodynamic response model for tolerance and rebound phenomena. *J. Pharm. Sci.* **87**, 1577– 1584 (1998).
18. Jacqmin, P. *et al.* Modelling response time profiles in the absence of drug concentrations: definition and performance evaluation of the K-PD model. *J. Pharmacokinet. Pharmacodyn.* **34**, 57– 85 (2007).
19. Bergstrand, M., Hooker, A.C., Wallin, J.E. & Karlsson, M.O. Prediction-corrected visual predictive checks for diagnosing nonlinear mixed-effects models. *AAPS J.* **13**, 143– 151 (2011).
20. Holford, N., Heo, Y.A. & Anderson, B. A pharmacokinetic standard for babies and adults. *J. Pharm. Sci.* **102**, 2941– 2952 (2013).
21. Lin, J.H. Pharmacokinetics of biotech drugs: peptides, proteins and monoclonal antibodies. *Curr. Drug Metab.* **10**, 661– 691 (2009).
22. Gao, W. & Jusko, W.J. Target-mediated pharmacokinetic and pharmacodynamic model of exendin-4 in rats, monkeys, and humans. *Drug Metab. Dispos.* **40**, 990–997 (2012).
23. Samtani, M.N., Perez-Ruixo, J.J., Brown, K.H., Cerneus, D. & Molloy, C.J. Pharmacokinetic and pharmacodynamic modeling of pegylated thrombopoietin mimetic peptide (PEG-TPOm) after single intravenous dose administration in healthy subjects. *J. Clin. Pharmacol.***49**, 336– 350 (2009).
24. Aiuti, A. *et al.* Human CD34(+) cells express CXCR4 and its ligand stromal cell-derived factor-1. Implications for infection by T-cell tropic human immunodeficiency virus. *Blood.* **94**, 62– 73 (1999).
25. Lack, N.A. *et al.* A pharmacokinetic-pharmacodynamic model for the mobilization of CD34+ hematopoietic progenitor cells by AMD3100. *Clin. Pharmacol. Ther.* **77**, 427–436 (2005).
26. Ozkan, M.C., Sahin. F, & Saydam, G. Peripheral blood stem cell mobilization from healthy donors. *Transfus. Apher. Sci.* **53**, 13– 16 (2015).
27. Neupogen [package insert]. Thousand Oaks (CA): Amgen Inc.; 2015 Available from: <http://www.accessdata.fda.gov/drugsatfda_docs/label/2015/103353s5186lbl.pdf>
28. Brugger, W. *et al.* Mobilization of peripheral blood progenitor cells by sequential administration of interleukin-3 and granulocyte-macrophage colony-stimulating factor following polychemotherapy with etoposide, ifosfamide, and cisplatin. *Blood.* **79**, 1193– 1200 (1992).
29. Paiva, B. *et al.* Detailed characterization of multiple myeloma circulating tumor cells shows unique phenotypic, cytogenetic, functional, and circadian distribution profile. *Blood.* **122**, 3591–3598 (2013).

Supplementary information accompanies this paper on the *CPT: Pharmacometrics & Systems Pharmacology* website (http://psp-journal.com)